J Biomol NMR (2012) 53:13–23
DOI 10.1007/s10858-012-9621-x

ARTICLE

Quantitative comparison of errors in ^{15}N transverse relaxation rates measured using various CPMG phasing schemes

Wazo Myint · Yufeng Cai · Celia A. Schiffer · Rieko Ishima

Received: 10 October 2011 / Accepted: 20 February 2012 / Published online: 1 April 2012

Abstract Nitrogen-15 Carr-Purcell-Meiboom-Gill (CPMG) transverse relaxation experiment are widely used to characterize protein backbone dynamics and chemical exchange parameters. Although an accurate value of the transverse relaxation rate, R_2, is needed for accurate characterization of dynamics, the uncertainty in the R_2 value depends on the experimental settings and the details of the data analysis itself. Here, we present an analysis of the impact of CPMG pulse phase alternation on the accuracy of the ^{15}N CPMG R_2. Our simulations show that R_2 can be obtained accurately for a relatively wide spectral width, either using the conventional phase cycle or using phase alternation when the r.f. pulse power is accurately calibrated. However, when the r.f. pulse is miscalibrated, the conventional CPMG experiment exhibits more significant uncertainties in R_2 caused by the off-resonance effect than does the phase alternation experiment. Our experiments show that this effect becomes manifest under the circumstance that the systematic error exceeds that arising from experimental noise. Furthermore, our results provide the means to estimate practical parameter settings that yield accurate values of ^{15}N transverse relaxation rates in the both CPMG experiments.

Keywords Relaxation · Monte Carlo · Dynamics · Protein · NMR · CPMG

W. Myint · R. Ishima (✉)
Department of Structural Biology, University of Pittsburgh School of Medicine, Rm 1037, Biomedical Science Tower 3, 3501 Fifth Avenue, Pittsburgh, PA 15260, USA
e-mail: ishima@pitt.edu

Y. Cai · C. A. Schiffer
Department of Biochemistry and Molecular Pharmacology, University of Massachusetts Medical School, 364 Plantation Street, Worcester, MA 01605, USA

Abbreviations

CPMG	Carr-Purcell-Meiboom-Gill
R_2	Transverse relaxation rate
R_2^{err}	Uncertainty of transverse relaxation rate
$\omega_{off}/2\pi$	Off-resonance frequency
r.f.	Radio frequency

Introduction

NMR relaxation is one of powerful methods to characterize internal motion of individual sites of proteins (Bruschweiler 2003; Dayie et al. 1996; Farrow et al. 1995; Fushman and Cowburn 2001; Igumenova et al. 2006; Ishima and Torchia 2000; Jarymowycz and Stone 2006; Kay 2005; Palmer 2001; Peng and Wagner 1995; Redfield 2004). Several relaxation rates, including the transverse relaxation rate (R_2), are typically used to characterize the degree of internal motion in biomolecules (Kay et al. 1989; Lipari and Szabo 1982a; Lipari and Szabo 1982b; Nirmala and Wagner 1988). R_2 is also used to detect slow conformational changes in biomolecules (Carver and Richards 1972; Davis et al. 1994; Ishima et al. 1998; Loria et al. 1999; Mulder et al. 1999; Orekhov et al. 1994). In biomolecular relaxation experiments, accurate error estimation is important in order to compare with NMR-derived dynamics parameters with those obtained by other methods, such as Gibbs free energy estimated from chemical exchange (Farrow et al. 1995; Huang and Oas 1995; Szyperski et al. 1993), molecular dynamics simulation data (Chandrasekhar et al. 1992; Eriksson et al. 1993; Horita et al. 2000; Smith et al. 1995; Wrabl et al. 2000; Yamasaki et al. 1995), and conformational entropy estimated from generalized order parameters (Akke and Palmer 1996; Li et al. 1996;

Yang and Kay 1996). The accuracy and precision of R_2 measurements, have been carefully analyzed (Bain et al. 2010, 2011; Bretthorst et al. 2005; Czisch et al. 1997; Ishima and Torchia 2005; Istratov and Vyvenko 1999; Korzhnev et al. 2000; Long et al. 2008; Myint et al. 2009; Palmer et al. 1991; Ross et al. 1997; Skelton et al. 1993; Viles et al. 2001; Yip and Zuiderweg 2004). However, some of the R_2 measurements remain unclear, yet.

One approach to improve the accuracy of R_2 measurements, by reducing cumulative pulse error, is an alternative phase scheme that applies pairs of orthogonal 180° pulses ($XXY\overline{Y}$) rather than the conventional CPMG ($XXXX$) (Bain et al. 2010, 2011; Gullion et al. 1990; Long et al. 2008; Yip and Zuiderweg 2004). The alternative phase scheme with a correction factor given to account for longitudinal relaxation during the pulsing was found to provide more accurate transverse relaxation rates covering a wider off-resonance frequency range than the conventional scheme (Bain et al. 2011; Yip and Zuiderweg 2004). This conclusion was supported by simulation results as well as experimental results. However, the studies assumed relatively low power radio-frequency (r.f.) pulses ($\sim$2.5 kHz), which is far smaller than in typical applications (Bain et al. 2011; Yip and Zuiderweg 2004). Although we and others have studied off-resonance errors (Bain et al. 2011; Czisch et al. 1997; Ishima and Torchia 2005; Korzhnev et al. 2000; Myint et al. 2009; Ross et al. 1997), quantitative analysis of the uncertainty of R_2 determine using the alternative CPMG phase scheme has not been studied. Most ^{15}N CPMG relaxation experiments applied to protein backbone dynamics studies have been performed using the conventional CPMG sequence (Meiboom and Gill 1958), and the practical advantage of the alternative phase scheme method has not yet been established.

The purpose of this article is to establish the condition under which the alternative phase scheme provides a practical advantage to the conventional CPMG scheme in measuring accurate R_2 values. In particular, we aim to identify whether it is advantageous or not when a relatively strong r.f. is employed for CPMG pulse train. In order to achieve this goal, we simulated ^{15}N CPMG relaxation data using three different phase schemes, and determined R_2 and its uncertainty for each as a function of off-resonance frequencies. The R_2 uncertainty was estimated by Monte Carlo error estimations in which a Gaussian distribution was assumed to generate synthetic datasets for the samplings. We generated the synthetic dataset by employing two different standard deviations (a) given by a rmsd deviation of the noise of the NMR spectra and (b) by a rmsd deviation of the residuals (I_i–I^{fit}) in the fit. Both have been used for ^{15}N relaxation data analysis (Nicholson et al. 1992; Palmer et al. 1991; Skelton et al. 1993). The former sampling reflects only the statistical noise uncertainties of R_2 but not any additional error. The latter reflects overall fit-uncertainties that include both experimental statistical noise and systematic errors. By comparing the R_2 uncertainties, magnitudes of the uncertainties other than those due to the experimental noise are estimated (Ishima and Torchia 2005). Our results show that in CPMG experiments performed by employing a radio-frequency of $B_1 > 5$ kHz, R_2 obtained using the conventional CPMG ($XXXX$) phase scheme is close to the one obtained using the alternative phase scheme ($XXY\overline{Y}$) at the off-resonance frequency, $\omega_{off}/2\pi$, up to 1,400 Hz. However, the conventional CPMG is expected to introduce higher systematic error even with $\omega_{off}/2\pi < 1{,}400$ Hz presumably due to non-exponential behavior of magnetization decay. We conducted ^{15}N CPMG relaxation experiments to verify the results of the calculations. Experimental results further showed that the differences in R_2 uncertainties in the two schemes are manifest only when the noise-to-signal ratio is significantly smaller than the fractional systematic error on R_2.

Methods

NMR Experiments

^{15}N transverse relaxation experiments were conducted using a 0.8 mM ^{15}N labeled ubiquitin at pH 4.5 on a Bruker Avance 900 NMR instrument. Ubiquitin sample was purchased and prepared as described previously (Myint et al. 2009). Three transverse relaxation experiments were performed with a conventional CPMG phase scheme ($XX - XX$, here noted 00-00), an alternative phase scheme ($XX - Y\overline{Y}$, here noted as 00-13), and a long alternative phase scheme ($XXY\overline{Y} - XXY\overline{Y}$, here noted as 0013-0013). Here, X and Y indicate pulse phases, and a hyphen indicates the timing applied to the ^{1}H 180° pulses to suppress cross-correlation by ^{1}H–^{15}N dipolar interaction and ^{15}N chemical shift anisotropy (CSA) (Kay et al. 1992; Palmer et al. 1992). We used the same CPMG pulse sequence that was applied previously ((Freedberg et al. 2002), except for an additional semi-constant time for the t_1 evolution, not in the original sequence (Kay et al. 1992). The total phase cycle is 8 with a phase inversion for the CPMG period. All the ^{15}N pulses are applied even number of times at each pulse scheme. Delays for the 00-00 and 00-13 experiments were varied: 0, 8, 16, 24, 32, 40, and 48 ms for the 00-00 and 00-13. Delays for the 0013-0013 experiments were varied: 0, 16, 32, and 48 ms. The maximum delay is set shorter than the expected $1/R_2$ because of the high sensitivity of an instrument equipped with a cryogenic probe and to avoid significant sample heating (Myint et al. 2009). Radio-frequency power for the ^{15}N pulses was 5.56 kHz (90 μs as a 180° pulse), and a half duration between ^{15}N

CPMG pulses, τ_{CP}, was 0.5 ms. Here, $2\tau_{CP}$ is the time between the centers of two adjacent CPMG pulses. ^{15}N pulses were applied at 130 ppm as a carrier frequency to investigate off-resonance effects. The number of scans was 8. Using the same pulse powers, ^{15}N longitudinal relaxation was recorded for the analysis of the 00-13 type relaxation data. The delays applied for the longitudinal relaxation measurements were: 0, 0.05, 0.1, 0.25, and 0.5 s.

^{15}N transverse relaxation experiments were also performed using a 250 μM Human Immunodeficiency virus-1 (HIV-1) protease at pH 5.8 on a Bruker Avance 600 MHz NMR instrument. The protease was over-expressed and purified mainly using the previous protocol (Nalam et al. 2007). Data was recorded using a conventional CPMG phase scheme ($XX - XX$) with delays of 0, 8, 16, 24, 32, 48, and 64 ms. Data were recorded by employing the same r.f. field strength for the ^{15}N pulses, 5.56 kHz, as the same that of 900 MHz. However, the carrier frequency of the pulse was placed at 117 ppm that is approximately the center of the amide ^{15}N chemical shifts of the protease sample. 64 scans were accumulated for each free induction decay.

Data analysis

Free induction decay signals were zero-filled four times, apodized with a sine window function with 40 % offset, and Fourier transformed in both dimensions using NMRpipe software (Delaglio et al. 1995). Signal intensities at individual positions were taken instead of peak volumes using the NMRdraw software (Delaglio et al. 1995). Lineshape fitting algorithm was not used to estimate peak heights. Experimental noise was obtained for each two-dimensional spectrum, but assumed to be the same in each CPMG experiments.

For each time-course of magnetization decay, a transverse relaxation rate, R_2, was optimized assuming a mono-exponential decay function, $I(t) = I_0\exp(-t\cdot R_2)$. In theory, if the initial intensity is correct, there is only one unknown parameter in this equation. However, since there is small loss of intensity at time zero, both I_0 and R_2 are typically optimized. Note that the same equation is used for R_1 determination as well as R_2 in protein ^{15}N NMR relaxation since the Freeman-Hill method is used (Freeman and Hill 1971).

Once R_2 values were optimized, Monte Carlo error estimation was performed to estimate uncertainty of R_2. In this method, first unknown parameters, R_2 and the initial intensity, were optimized using the experimental data, and the set of the fit "ideal" intensities were back-calculated using the optimized parameters. Second, a hundred number of sets of synthetic intensity data were generated to allow a Gaussian distribution with the ideal intensities as the mean. Finally, optimization was repeated for these synthesized data sets to calculate the standard deviation (SD) of R_2 and the initial intensity. The Gaussian distribution to generate synthetic intensities was defined in two ways:

(1) a root-mean-square deviation (rmsd) of the NMR spectral noise (Palmer et al. 1991; Skelton et al. 1993)
(2) a standard deviation of the residual (I_i–I^{fit}) of the fit (Nicholson et al. 1992).

In this article, R_2 errors that were calculated using the experimental noise are denoted $R_2^{noise\_err}$, and those were calculated using the residual of the fit are denoted $R_2^{fit\_err}$. The former reflects only experimental noise error and the later reflects overall fit-uncertainties that include both experimental statistic noise and systematic noise. By comparing the two types of R_2 uncertainties the uncertainties other than those due the experimental noise are estimated (Ishima and Torchia 2005).

The error in the R_2 value, measured using the 00-13 and 0013-0013 sequences, caused by R_1 relaxation during the r.f. pulses is recommended to be corrected using the equation introduced by Zuiderweg's group (Yip and Zuiderweg 2004):

$$R_2^{obs} = R_2 + d(R_1 - R_2)/4 = R_2(1 - d/4) + dR_1/4 \quad (1)$$

Here, d indicates a duty cycle of the r.f. pulse: total duration of the r.f. pulses divided by the entire CPMG delay. However, in the following analysis, no correction was made because the correction factor is calculated to be small. When pulse power $\gamma_N B_1/2\pi = 5.6$ kHz is applied with a reasonable delay ($\tau_{CP} = 0.45$ and 0.5 ms for simulation and experiments, respectively), the observed R_2 will be only 2.5 and 2.25 % smaller than the correct R_2, respectively when $R_1 = 0$ (Eq. 1). When $0 < R_1 < R_2$, the difference becomes less than 2.5 and 2.25 %, respectively. This is in contrast to the condition that was used by Yip and Zuiderweg in which ca. 8 % correction of R_2 was needed (Yip and Zuiderweg 2004). Note that since this equation does not contain any off-resonance frequency, some of the error caused by the combination of the effects of pulse imperfection and off-resonance is not corrected by this equation. We did not use the 00130031 sequence (Yip and Zuiderweg 2004) because the minimum cycle, each CPMG loop ($n = 1$) of $(00130031\text{-}00130031)_2$, needed to suppress cross correlation between ^{15}N CSA and ^{1}H–^{15}N dipolar interactions is long, i.e., 32 ms when $\tau_{CP} = 0.5$ ms.

Simulation

The time evolution of bulk nuclear magnetization of a scalar-coupled ^{15}N–^{1}H spin system was calculated to determine transverse relaxation rates. For this, we used a

relaxation matrix that contains 16 Cartesian product operators as the base set, as described previously (Allard et al. 1997; Allard et al. 1998; Myint et al. 2009; Myint and Ishima 2009).

E/2	N_X	N_Y	N_Z	H_X	H_Y	H_Z	$2N_XH_X$
$2N_YH_X$	$2N_ZH_X$	$2N_XH_Y$	$2N_YH_Y$	$2N_ZH_Y$	$2N_XH_Z$	$2N_YH_Z$	$2N_ZH_Z$

Time dependence of the relaxation was calculated step by step for each time increment, t_1, by solving the $M(t_0 + t_1) = \exp(R_2{*}t_1)M(t_0)$. τ_{CP} is 0.45 ms, and each CPMG loop of $(\tau'_{CP} - 180_N - \tau'_{CP} - \tau'_{CP} - 180_N - \tau''_{CP} - 180_H - \tau''_{CP} - 180_N - \tau'_{CP} - \tau'_{CP} - 180_N - \tau'_{CP})_2$ was set to be a 7.2 ms, and incremented to a total 72 ms. Here, τ'_{CP} and τ''_{CP} satisfy $\tau_{CP} = \tau'_{CP} + 90_N$ and $\tau_{CP} = \tau''_{CP} + 90_N + 90_H$. Simulation was done twice with the starting ^{15}N transverse magnetization at X and $-X$ and detection at X and $-X$, respectively, for the phase cycle. The output is the average time course of the two phase cycles. In the relaxation matrix, ^1H and ^{15}N chemical shift and the 90-Hz ^1H–^{15}N J-coupling evolution, r.f. pulse effects, auto and cross relaxation terms, and cross-correlation terms were included (Allard et al. 1997; Allard et al. 1998; Myint et al. 2009; Myint and Ishima 2009). In the calculation, ^{15}N and ^1H r.f. pulses were applied at field strengths of 5.56 and 25 kHz, respectively, and ^{15}N signal off-resonance frequency, $\omega_{off}/2\pi$, was varied from $-3{,}000$ to 3,000 Hz in 200 Hz steps. Off-resonance frequency of the ^1H signal was set at 2,250 Hz, which corresponds to 7.5 ppm at 900 MHz NMR from the water resonance. Relaxation terms in the matrix were calculated assuming a simple Lorentzian spectral density function with a 5 ns rotational correlation time, 170 ppm ^{15}N CSA, and 1.02 Å N–H distance. Additional ^1H longitudinal and transverse relaxation rates of 10 and 20 s^{-1} were added, in addition to the ^1H–^{15}N dipolar term, to the ^1H relaxation (Myint et al. 2009).

Once the time dependence was calculated, R_2 and its uncertainty, $R_2^{fit\_err}$, were determined by Monte-Carlo error estimation using the SD of the residual (I_i–I^{fit}) of the fit as the uncertainty in I_i (Nicholson et al. 1992). $R_2^{noise\_err}$ was not calculated because experimental noise itself was not assumed in the simulation. The effect of the inhomogeneity of the B_1 field was simulated by assuming that relative magnetization intensities of 0.375, 0.5, and 0.125 experienced respective r,f, field strengths of $1.0B_1$, $1.05B_1$ and $1.1B_1$, respectively, where B_1 is the correctly calibrated field strength. Then, R_2 and $R_2^{fit\_err}$ were determined from simulations of the weighted time course of the average magnetization. The simulation analysis for B_1 inhomogeneity was performed for the [00-00] and the [00-13] schemes individually. Calculations were performed using MATLAB software (The Mathworks Inc., Natick, MA, USA).

Results and discussions

The purpose of this study is to further identify systematic errors, that persist even when experiments are repeated (Bevington and Robinson 1992; Heinrich and Lyons 2007), in ^{15}N transverse relaxation rates, which are used to characterize protein backbone dynamics. In particular, uncertainties in CPMG R_2 values caused by systematic errors present when using phase schemes, [00-00], [00-13], and [0013-0013] are compared. For this purpose, we will firstly compare values of R_2 and $R_2^{fit\_err}$ derived from simulations of measurments obtained using phase-schemes, [00-00] and [00-13]. Next, we will compare experimental results obtained using the [00-00], [00-13], and [0013-0013] schemes. In the evaluation of the experimental results, R_2 errors estimated from two sets of Monte-Carlo methods, $R_2^{fit\_err}$ and $R_2^{noise\_err}$, are compared as well as the R_2 values to idenity systematic errors.

Simulated off-resonance frequency dependence of [00-00] and [00-13] at a practical r.f. power level

The time course of magnetization in a scalar-coupled two-spin system was calculated for the conventional phase [00-00] and the alternative phase [00-13], using r.f. pulse power of $\gamma_N B_1/2\pi = 5.6$ kHz (i.e., 90 μs, 180° pulse) at varying off-resonance frequency, $\omega_{off}/2\pi$. Time courses of magnetization obtained by employing the [00-00] scheme at $\omega_{off}/2\pi = \pm$ 2,400 Hz exhibit non single-exponential decay profiles (Fig. 1a). The profiles are basically consistent to the previous results [For example, Fig. 4 of the reference, (Yip and Zuiderweg 2004)]. In contrast, the time course of magnetization obtained by employing the [00-13] scheme under the same conditions exhibited profiles that are closer to a single-exponential decay (Fig. 1b). This result is also consistent with previous observations (Bain et al. 2011; Yip and Zuiderweg 2004). Note that our simulation shows slightly different profiles at positive and negative $\omega_{off}/2\pi$. Such a different is not observed in the simulation for a single spin system, or when ^1H signal is located at the r.f. carrier frequency in the two-spin system (data not shown). Thus, although an even number of ^1H pulses is applied in each CPMG cycle, the difference in profiles is most likely due to an asymmetry caused by an ^1H off-resonance effect. The effect of the coupled spin was not taken into account in the previous CPMG simulations for the alternative phase schemes (Bain et al. 2011; Yip and Zuiderweg 2004).

Once the time course of magnetization was simulated, R_2 was determined by assuming that each time course decayed as a single-exponential function. The resultant R_2 values are shown as a function of the absolute value of $\omega_{off}/2\pi$ in Fig. 2a. R_2 values were determined using both

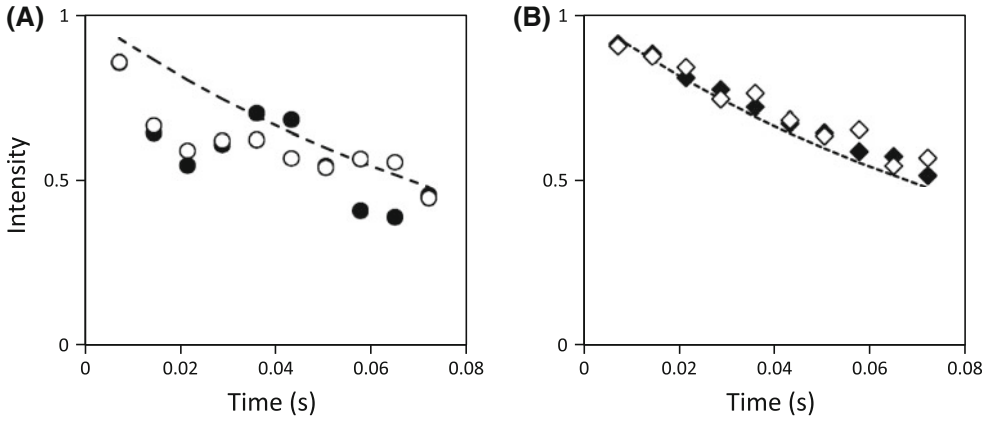

Fig. 1 Simulated time course of transverse magnetization using (**a**) the [00-00] sequence (*circles*) and (**b**) the [00-13] sequences (*diamonds*). In each figure, calculations were performed with $\omega_{off}/2\pi$ set equal to +2,400 Hz (*open symbols*) and −2,400 Hz (*closed symbols*)

[00-00] and [00-13] schemes and are denoted as $R_2^{00\text{-}00}$ and $R_2^{00\text{-}13}$, respectively. Both R_2 values were quite similar up to an off-resonance frequency, $\omega_{off}/2\pi = 1{,}400$ Hz (i.e., $\omega_{off}/(\gamma_N B_1) = 0.25$), with average difference in R_2 1.2 % and with the maximum difference in R_2 of 2.2 % (Fig. 2a). Within each individual scheme, the fractional root-mean square deviations of R_2 values in the range from $\omega_{off}/2\pi$ 0 to 1,400 Hz were 0.20 % and 0.17 % for $R_2^{00\text{-}00}$ and $R_2^{00\text{-}13}$, respectively. These results were obtained including all data except for the $R_2^{00\text{-}00}$ point at 1,200 Hz. As shown by an arrow in Fig. 2a, the $R_2^{00\text{-}00}$ at 1,200 Hz was significantly higher than others. When the magnetization along X-axis starts CPMG duration and the pulses are applied from the X-axis, the Y-component of the transverse magnetization vector rotates through the Y–Z plane during the pulsing whereas the X-component stays mostly in the transverse plane. Thus, pulse imperfection effect caused by chemical shift precession during the pulsing becomes largest when a magnetization vector undergoes almost 360° precession between the adjacent CPMG pulses, as has been shown in other simulation and experimental results (Bain et al. 2011; Yip and Zuiderweg 2004).

At $\omega_{off}/2\pi > 1{,}400$ Hz, deviations of R_2 by the off-resonance effects are observable in both $R_2^{00\text{-}00}$ and $R_2^{00\text{-}13}$ (Fig. 2). In previous results, $R_2^{00\text{-}13}$ profiles were reported to exhibit a smaller and smoother change than those of $R_2^{00\text{-}00}$ (Bain et al. 2011; Yip and Zuiderweg 2004). This discrepancy between these results and ours is mostly caused by differences in experimental and simulation parameter: their applied B_1 field strength ($\gamma_N B_1/2\pi \leq 2.5$ kHz) was smaller than that of ours ($\gamma_N B_1/2\pi = 5.6$ kHz), and their τ_{CP} (0.35 ms) was shorter than ours (0.45 and 0.5 ms). The latter set of the parameters, the weaker B_1, make the [00-00] profile unfavorable. In addition, even in the previous experimental results, reduced but clear deviations of R_2 caused by off-resonance effects were shown even in $R_2^{00\text{-}13}$ (Bain et al. 2011; Yip and Zuiderweg 2004). Errors in $R_2^{00\text{-}13}$ found at a large $\omega_{off}/2\pi$ values are not corrected by Eq. (1) because Eq. (1) does not contain off-resonance frequency as one of calibration parameters. Overall, using our practical

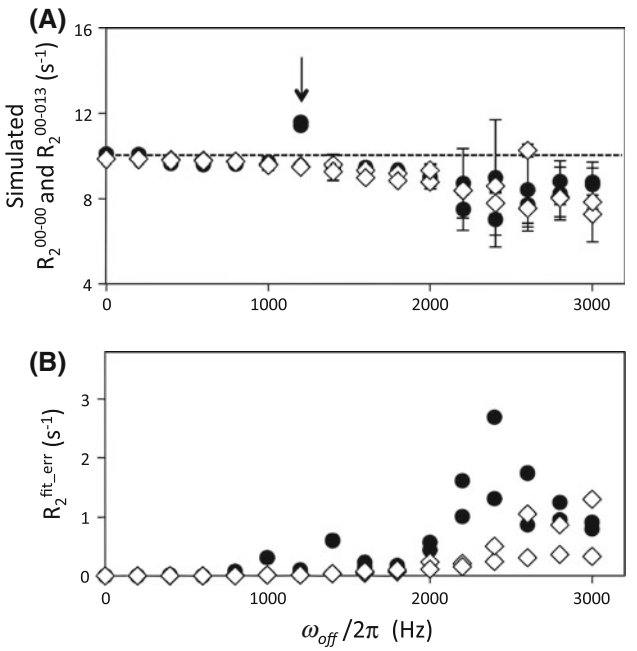

Fig. 2 (**a**) Transverse relaxation rate, R_2, and (**b**) its error, $R_2^{fit\_err}$, determined by simulation using the [00-00] (*filled circles*) and the [00-13] (*open diamonds*) sequences, plotted as a function of the absolute off-resonance frequency, $\omega_{off}/2\pi$. Simulation of the time dependence of magnetization was performed varying $\omega_{off}/2\pi$ from −3,000 to 3,000 Hz at a 200 Hz step. Note that there are two data points determined using each pulse scheme at each $\omega_{off}/2\pi$ point, i.e., at the positive and the negative frequencies (Here, the two data points are shown by the same *symbols*). The *arrow* in (**a**) indicates a data point at a frequency that is close to the inverse of the CPMG pulse duration, a condition in which magnetization undergoes almost 360° precession during the period between the two adjacent CPMG pulses (see text). In (**a**), the *dashed line* indicates the original R_2 determined only by the auto relaxation. R_2 values are all plotted with $R_2^{fit\_err}$ as the error bars, while some of the error bars may not be notably large. $R_2^{fit_err}$s were estimated from the residual of the fits (see "Methods" section)

conditions for ^{15}N relaxation measurements, $R_2^{00\text{-}00}$ and $R_2^{00\text{-}13}$ exhibit similar profiles almost within the entire experimentally required $\omega_{off}/2\pi$ range.

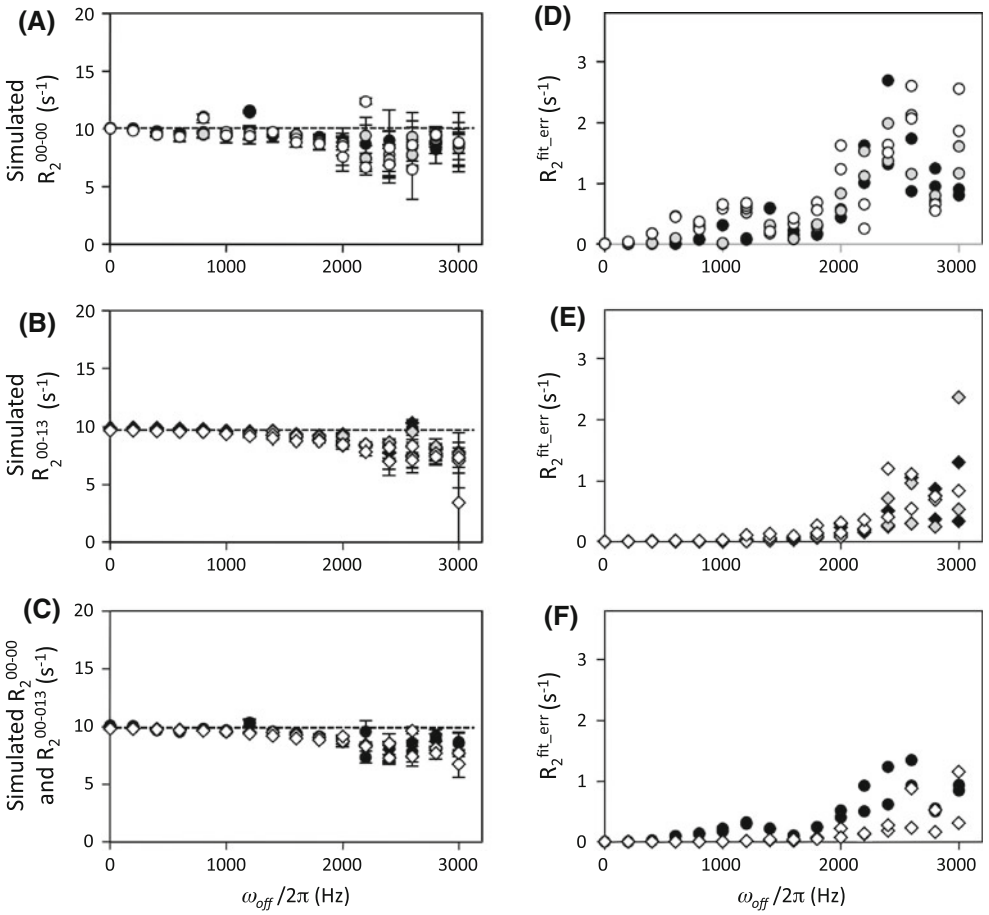

Fig. 3 (**a**, **b**, **c**) Transverse relaxation rate, R_2, and (**d**, **e**, **f**) its error, $R_2^{fit\_err}$, determined by simulation, plotted as a function of the off-resonance frequency, $\omega_{off}/2\pi$. Simulation was performed (**a**, **d**) using the [00-00] scheme, (**b**, **e**) using the [00-13] scheme, and (**c**, **f**) assuming the B_1 inhomogeneity for both. In all figures, *circle* and *diamond* symbols indicate for R_2 obtained using the [00-00] and the [00-13] schemes, respectively. In (**a**, **b**, **d**, **e**), simulation of the time dependence of magnetization was done at a correctly calibrated B_1 field strength of 5.56 kHz CPMG 180° pulse of 90 μs (*filled symbols*), at a 5 % stronger B_1 field strength (*gray symbols*), and at a 10 % stronger B_1 field strength (*open symbols*). In (**c**) and (**f**), R_2 and $R_2^{fit\_err}$ determination assuming B_1 inhomogeneity was performed for both of the [00-00] and the [00-13] schemes (see Methods section). In the calculation, $\omega_{off}/2\pi$ was varied from −3,000 to 3,000 Hz at a 200 Hz step. There are two data points determined using each condition at each $\omega_{off}/2\pi$, i.e., at the positive and the negative frequencies. In (**a**–**c**), R_2 values are all plotted with $R_2^{fit\_err}$ as the error bars while some of the error bars may not be notably large

Uncertainty of each R_2 value, $R_2^{fit\_err}$, was estimated from the Monte-Carlo method by assuming an average residual of the simulated intensities from the fit-intensities as a SD for the normal distribution (Fig. 2b). This $R_2^{fit\_err}$ solely reflects a discrepancy from a single-exponential decay model. $R_2^{fit\_err}$ for R_2^{00-13} exhibits very small uncertainties (<0.1 s^{-1} that correspond to < 1% of R_2^{00-13}) in the entire $\omega_{off}/2\pi$ range. In contrast, $R_2^{fit\_err}$ obtained for R_2^{00-00} exhibited large uncertainties at $\omega_{off}/2\pi > 1{,}800$ Hz, reflecting non-exponential behavior of magnetization simulated using the [00–00] scheme (Fig. 2b). Nevertheless, $R_2^{fit\_err}$ values for R_2^{00-00} (<2%) remained small for $\omega_{off}/2\pi < 1{,}800$ Hz. Again this frequency range covers nearly all ^{15}N signals of backbone amides in diamagnetic proteins up to 20 ppm at a 91 MHz ^{15}N resonance frequency (Fig. 2b). Overall, application of the practical B_1 field strength ($\gamma_N B_1/2\pi = 5.6$ kHz) provides similar R_2 values in both R_2^{00-00} and R_2^{00-13} schemes, within the spectral range of ±1,400 Hz.

Effects of pulse strength miscalibration on R_2 error, determined by simulation

Similar simulations of magnetization and the determinations of R_2 were performed by varying the B_1 field strength and keeping the pulse width constant (i.e., power miscalibration). At a 5 or 10 % increase (miscalibration) of the B_1 field strength, R_2^{00-00} exhibits more variation of R_2 values at $\omega_{off}/2\pi < 1{,}400$ Hz (Fig. 3a), which is larger than the variation of R_2^{00-13} (Fig. 3b). Similar to these observations, but more

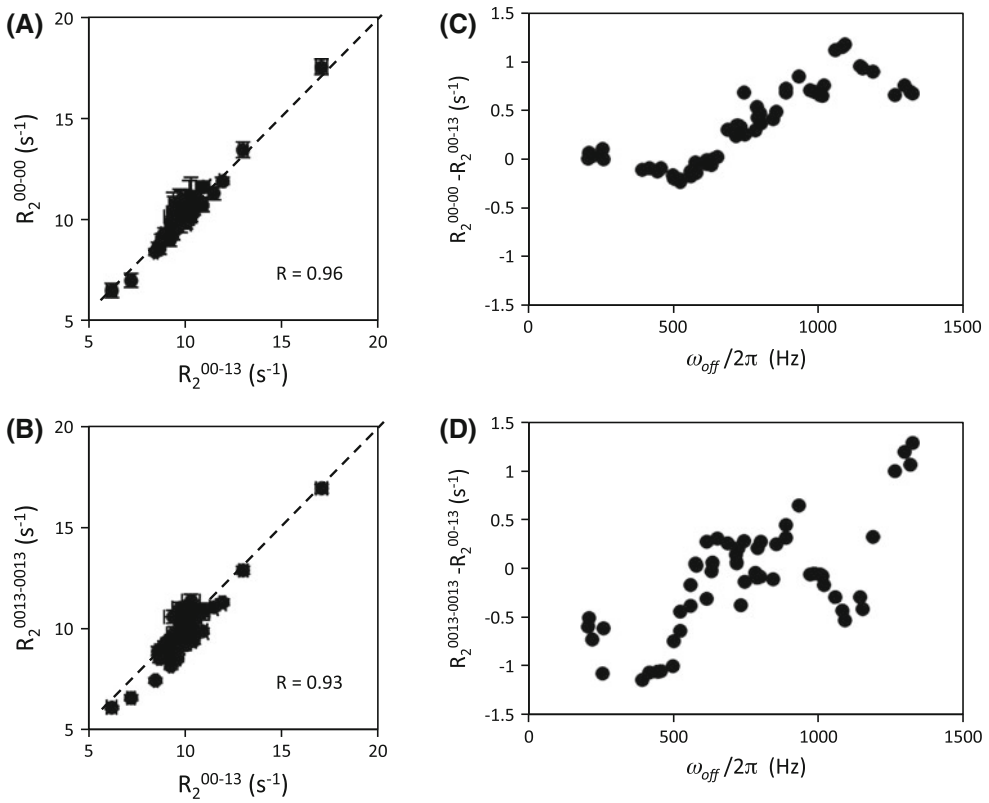

Fig. 4 Transverse relaxation rate, R_2, for ubiquitin experimentally determined using the [00-13] sequence was compared with (**a**) those obtained using the conventional [00-00] sequence and (**b**) those obtained using the [0013-0013] sequence using a 900 MHz NMR instrument. Difference of (**c**) the rates determined between the [00-00] and the [00-13] schemes, and (**d**) between the [0013-0013] and the [00-13] schemes are shown as a function of the off-resonance frequency, $\omega_{off}/2\pi$. Note that the number of relaxation data points corrected for the [0013-0013] sequence were smaller than those of [00-00] and [00-13] due to the longer cycle length. For this reason, a [00130031-00130031] sequence (Yip and Zuiderweg 2004) was not applied. Only the data points at $\omega_{off}/2\pi < 1{,}500$ Hz were include because large error bars at larger resonance off-sets make it difficult to view the correlation plots. In (**a**) and (**b**), R_2 values are all plotted with $R_2^{fit\_err}$ error bars but may not be notable when the errors are small

significantly, $R_2^{fit\_err}$ for $R_2^{00\text{-}00}$ (Fig. 3d) became larger than that of $R_2^{00\text{-}13}$ at the miscalibrated B_1 field strength (Fig. 3e). In particular, the $R_2^{fit\_err}$ for $R_2^{00\text{-}00}$ increased in proportion to the power miscalibration (Fig. 3d). Such differences between $R_2^{00\text{-}00}$ and $R_2^{00\text{-}13}$, and between $R_2^{fit\_err}$ for $R_2^{00\text{-}00}$ and $R_2^{fit\_err}$ for $R_2^{00\text{-}13}$ are reduced when B_1 inhomogeneity is taken into account in the simulations (Fig. 3c, f). Overall, the simulations demonstrate that the difference between R_2 obtained using $R_2^{00\text{-}00}$ and $R_2^{00\text{-}13}$ is insignificant for a relatively wide spectral width, provided that r.f. pulses are properly calibrated (Fig, 2). However, the difference becames significant when r.f. pulses are miscalibrated (Fig. 3). In particular, the [00-13] scheme is more tolerant to miscalibration errors than the [00-00] scheme.

Experimental R_2 determined using [00-00], [00-13], and [0013-0013] sequences

To verify the predictions of these simulations, we conducted ^{15}N R_2 experiments for ubiquitin using a 900 MHz NMR instrument, and evaluated experimental results only for signals that were fit by an single-exponential decay function with $R_2^{err} < 1\ s^{-1}$ (Fig. 4). Most of the $R_2^{00\text{-}00}$ values were very similar to $R_2^{00\text{-}13}$ values (Fig. 4a). As shown in Fig. 4c, $R_2^{00\text{-}00}$ and $R_2^{00\text{-}13}$ did not exhibit significant difference for signals at $\omega_{off}/2\pi < 500$ Hz, but the R_2 values increaslingly differ as $\omega_{off}/2\pi$ (off-resonance) increases. In contrast, although the effect of resonance offset for $R_2^{0013\text{-}0013}$ is basically similar to that of $R_2^{00\text{-}13}$ (Fig. 4b), $R_2^{0013\text{-}0013}$ exhibits differences from $R_2^{00\text{-}13}$ even when, $\omega_{off}/2\pi < 500$ Hz (Fig. 4d). Since the [0013-0013] scheme is more symmetric with respect to the ^1H 180° pulses than the [00-13] scheme, a possible explanation of the poor performance of the [0013-0013] scheme when $\omega_{off}/2\pi$ is small may be incomplete suppression of CSA-dipolar cross correlation. In the [0013-0013] scheme the period between ^1H 180° pulses is twice that of [00-13] scheme. As shown previously (Kay et al. 1992; Palmer et al. 1992), the cross correlation is suppressed in a two-spin system. However, artifacts in R_2 measurements may

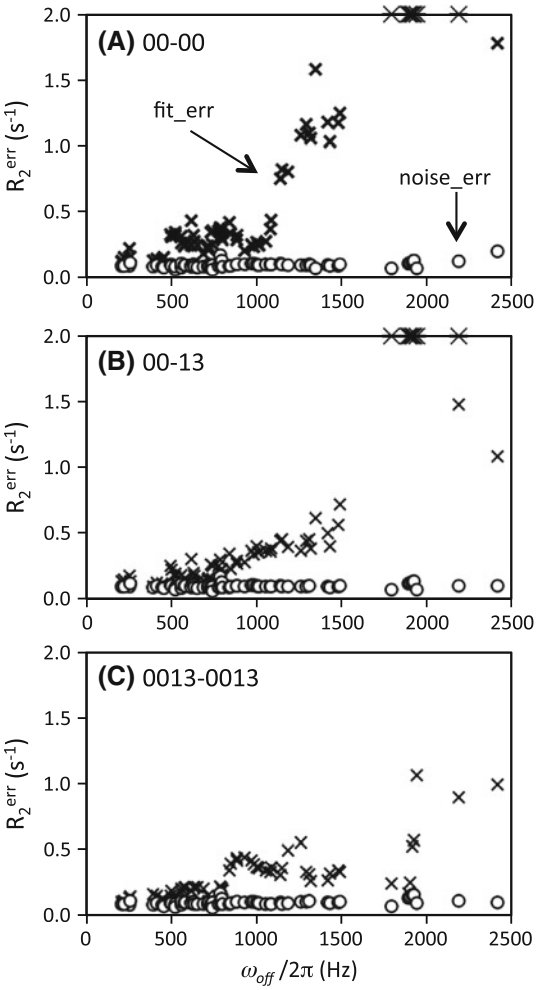

Fig. 5 Uncertainties, R_2^{err}, of the transverse relaxation rates for ubiquitin experimentally determined using (**a**) [00-00], (**b**) [00-13], and (**c**) [0013-0013] sequences on a 900 MHz NMR instrument, shown as a function of the off-resonance frequency, $\omega_{off}/2\pi$. R_2 values that are shown in Fig. 4 are used. An additional 16 sets of data that exhibited $R_2^{err} > 1\ s^{-1}$ were also included in the graphs in order to show how the uncertainty increases as a function of $\omega_{off}/2\pi$. R_2^{err} values were determined by two different Monte-Carlo error estimations in which the SDs of a Gaussian distribution function that generates synthetic data sets were given by rmsd of spectral noise, $R_2^{noise\_err}$ (*circle*), and by rmsd of residuals of the initial fit intensities, $R_2^{fit\_err}$ (×-symbols). Difference of the two uncertainties indicates errors other than experimental noise. R_2^{err} values above 2 s^{-1} are shown as the ceiling values

become significant because of the interactions with external protons that have been neglected in our simulations.

Monte-Carlo error estimation was calculated for ubiquitin R_2 values in two ways: using the spectral noise ($R_2^{noise\_err}$) and using the residual of the fits ($R_2^{fit\_err}$), to generate the synthetic data. Since ubiquitin is a rigid, small protein, amide signal heights were quite uniform (except for E24 that undergoes chemical exchange and exhibits severe line broadening at 900 MHz) as is evident in the R_2 correlations plotted in Fig. 4. Therefore, $R_2^{noise\_err}$ was approximately the same for all three datasets (Fig. 5, circles). In contrast, $R_2^{fit\_err}$ exhibits a quite different profile for $R_2^{00\text{-}00}$ (Fig. 5a, × -symbols) compared with $R_2^{00\text{-}13}$ and $R_2^{0013\text{-}0013}$ (Fig. 5b, c, × -symbols). $R_2^{fit\_err}$ for $R_2^{00\text{-}00}$ begins to increase at $\omega_{off}/2\pi$ ca. 1,000 Hz, and becomes over 2 s^{-1} at $\omega_{off}/2\pi > 1{,}800$ Hz (Fig. 5a, × -symbols). This profile is consistent with the simulations that incorporate the effect of pulse miscalibration, Fig. 3f, demonstrating the excellent performance of the calculations. $R_2^{fit\_err}$ for $R_2^{00\text{-}13}$ and $R_2^{0013\text{-}0013}$ exhibits a more gradual increases as a function of $\omega_{off}/2\pi$, and stays smaller than $R_2^{fit\_err}$ for $R_2^{00\text{-}00}$ even at $\omega_{off}/2\pi \sim 1{,}500$ Hz. This small gradual increase of R_2^{err} for the phase alternation experiments is also consistent with the simulation results, Fig. 3f. Overall, in both $R_2^{00\text{-}00}$ and $R_2^{00\text{-}13}$, $R_2^{fit\_err}$ almost equals $R_2^{noise\_err}$ when $\omega_{off}/2\pi$ is small, and increases as $\omega_{off}/2\pi$ increases. This increasing discrepancy between the $R_2^{fit\_err}$ and $R_2^{noise\_err}$ as $\omega_{off}/2\pi$ increases is clear evidence of the off-resonance related systematic error.

Off-resonance systematic error is not observed in large proteins

To test if off-resonance effects are observable in the case of a larger protein with less spectra sensitivity than ubiquition, the CPMG experiments were also performed for HIV-1 protease using a 600 MHz instrument. In this experiment, the ^{15}N pulse carrier was placed at 117 ppm which is almost the center of the ^{15}N chemical shifts of the protease backbone amides. $R_2^{00\text{-}00}$ for the 92 residues are on average 15.2 s^{-1} (±2.1 s^{-1}), which is approximately 1.5 times larger than that of ubiquitin and consistent with previous protease measurements (Freedberg et al. 2002). $R_2^{00\text{-}00}$ values are relatively uniform in this $\omega_{off}/2\pi$ range (Fig. 6a). $R_2^{noise\_err}$ is 0.17 s^{-1} whereas $R_2^{fit\_err}$ is 0.22 s^{-1} (Fig. 6b). The $R_2^{noise\_err}$ values are approximately 2 % of R_2^{00-00}. Although some $R_2^{fit\_err}$ are higher at $\omega_{off}/2\pi > 500$ Hz, the differences between $R_2^{noise\_err}$ and $R_2^{fit\_err}$ are not significant. Thus, differences in R_2^{err} estimated by two methods are not observed because the noise error is larger than the off-resonance error. This result is in contrast to that obtained for ubiquitin.

Summary

In this study, ^{15}N CPMG experiments with and without the phase alternation were investigated at the practical high pulse power ($\gamma_N B_1/2\pi = 5.6$ kHz) and also with ^1H 180° pulses that are applied to suppress dipolar/CSA cross correlation. Since CPMG performance is determined by the field strength of the r.f. pulse ($\gamma_N B_1/2\pi$), the delay between the CPMG pulses (τ_{CP}), the off-resonance frequency ($\omega_{off}/2\pi$), and relaxation rates and scalar couplings,

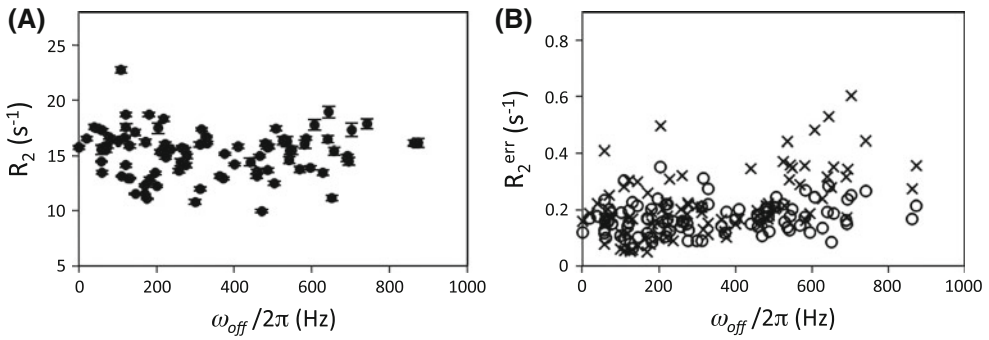

Fig. 6 (**a**) Transverse relaxation rate, R_2, and (**b**) its uncertainty, R_2^{err}, for HIV-1 protease experimentally determined using the [00-00] sequence on a 600 MHz NMR instrument with 117 ppm as ^{15}N pulse carrier frequency. In (**a**), R_2 values are all plotted with $R_2^{fit\_err}$ error bars but may not be notable when the errors are small. In (**b**), R_2^{err} values were determined by two different Monte-Carlo error estimations in which the SDs of a Gaussian distribution function that generates synthetic data sets were given by rmsd of spectral noise, $R_2^{noise\_err}$ (*circle*), and by rmsd of residuals of the initial fit intensities, $R_2^{fit\_err}$ (×-symbols)

it is important to investigate the performance at optimal parameter settings. First, our results showed that, in the high power condition, both pulse phase schemes yield similar results unless resonance off-sets are very large. Our simulations reproduced the reduction of the measurement accuracy as $\omega_{off}/2\pi$ increases even with the phase alternation method, which is consistent with the experimental results. Second, when the pulse power is miscalibrated, the fit error becomes larger in the conventional CPMG than the phase alternation approach, even when the resonance off-set is small. Third, although the full (longer) phase alternation cycle has a better performance in theory, our experimental results show that the actual performance of the longer cycle was not improved in the ^{15}N experiments with ^{1}H 180° pulses.

Acknowledgments We thank Dennis Torchia for useful discussions and critical reading of the manuscript. This study was financially supported by the American Heart Association (Great Rivers affiliate) new investigator grant 0765348U, National Science Foundation research grant MCB 0814905, and subcontract of National Institutes of Health program project 5P01GM066524-08.

References

Akke M, Palmer AG III (1996) Monitoring macromolecular motions on microsecond to millisecond time scales by $R1\rho - R1$ constant relaxation time NMR spectroscopy. J Am Chem Soc 118:911–912

Allard P, Helgstrand M, Hard T (1997) A method for simulation of NOESY, ROESY, and off-resonance ROESY spectra. J Magn Reson 129:19–29

Allard P, Helgstrand M, Hard T (1998) The complete homogeneous master equation for a heteronuclear two-spin system in the basis of Cartesian product operators. J Magn Reson 134:7–16

Bain AD, Anand CK, Nie Z (2010) Exact solution to the Bloch equations and application to the Hahn echo. J Magn Reson 206:227–240

Bain AD, Anand CK, Nie Z (2011) Exact solution of the CPMG pulse sequence with phase variation down the echo train: application to R2 measurements. J Magn Reson 209:183–194

Bevington PR, Robinson DK (1992) Data reduction and error analysis for the physical sciences. McGraw-Hill, New York

Bretthorst GL, Hutton WC, Garbow JR, Ackerman JJH (2005) Exponential parameter estimation (in NMR) using Bayesian probability theory. Concepts Magn Reson 27A:55–63

Bruschweiler R (2003) New approaches to the dynamic interpretation and prediction of NMR relaxation data from proteins. Curr Opin Struct Biol 13:175–183

Carver JP, Richards RE (1972) General 2-site solution for chemical exchange produced dependence of T2 upon carr-purcell pulse separation. J Magn Reson 6:89–105

Chandrasekhar I, Clore GM, Szabo A, Gronenborn AM, Brooks BR (1992) A 500 ps molecular dynamics simulation study of interleukin-1 beta in water. Correlation with nuclear magnetic resonance spectroscopy and crystallography. J Mol Biol 226:239–250

Czisch M, King GC, Ross A (1997) Removal of systematic errors associated with off-resonance oscillations in T2 measurements. J Magn Reson 126:154–157

Davis DG, Perlman ME, London RE (1994) Direct measurements of the dissociation-rate constant for inhibitor-enzyme complexes Via the T-1-Rho and T-2 (Cpmg) methods. J Magn Reson, Ser B 104:266–275

Dayie KT, Wagner G, Lefevre JF (1996) Theory and practice of nuclear spin relaxation in proteins. Annu Rev Phys Chem 47:243–282

Delaglio F, Grzesiek S, Vuister GW, Zhu G, Pfeifer J, Bax A (1995) Nmrpipe—a multidimensional spectral processing system based on Unix pipes. J Biomol NMR 6:277–293

Eriksson MA, Berglund H, Härd T, Nilsson L (1993) A comparison of 15 N NMR relaxation measurements with a molecular dynamics simulation: backbone dynamics of the glucocorticoid receptor DNA-binding domain. Proteins 17:375–390

Farrow NA, Zhang O, Forman-Kay JD, Kay LE (1995) Comparison of the backbone dynamics of a folded and an unfolded SH3 domain existing in equilibrium in aqueous buffer. Biochemistry 34:868–878

Freedberg DI, Ishima R, Jacob J, Wang YX, Kustanovich I, Louis JM, Torchia DA (2002) Rapid structural fluctuations of the free HIV protease flaps in solution. Protein Sci 11:221–232

Freeman R, Hill HDW (1971) Fourier transform study of NMR spin-lattic relaxation by "Progressive Saturation". J Chem Phys 54:3367–3377

Fushman D, Cowburn D (2001) Nuclear magnetic resonance relaxation in determination of residue-specific 15N chemical shift tensors in proteins in solution: protein dynamics and structure,

and applications of transverse relaxation optimized spectroscopy. In: James TL, Dötsch V, Schmitz U (eds) Nuclear magnetic resonance of biological macromolecules (Methods in Enzymology), vol 339. Academic Press, pp 109–126

Gullion T, Baker DB, Conradi MS (1990) New, compensated carr-purcell sequences. J Magn Reson 89:479–484

Heinrich J, Lyons L (2007) Systematic errors. Ann Rev Nucl Part Sci 57:145–169

Horita DA, Zhang W, Smithgall TE, Gmeiner WH, Byrd RA (2000) Dynamics of the Hck-SH3 domain: comparison of experiment with multiple molecular dynamics simulations. Protein Sci 9:95–103

Huang GS, Oas TG (1995) Submillisecond folding of monomeric lambda repressor. Proc Natl Acad Sci USA 92:6878–6882

Igumenova TI, Frederick KK, Wand AJ (2006) Characterization of the fast dynamics of protein amino acid side chains using NMR relaxation in solution. Chem Rev 106:1672–1699

Ishima R, Torchia DA (2000) Protein dynamics from NMR. Nat Struct Biol 7:740–743

Ishima R, Torchia DA (2005) Error estimation and global fitting in transverse-relaxation dispersion. J Biomol NMR 32:41–54

Ishima R, Wingfield PT, Stahl SJ, Kaufman JD, Torchia DA (1998) Using amide H-1 and N-15 transverse relaxation to detect millisecond time-scale motions in perdeuterated proteins: application to HIV-1 protease. J Am Chem Soc 120:10534–10542

Istratov AA, Vyvenko OF (1999) Exponential analysis in physical phenomena. Rev Sci Instrum 70:1233–1257

Jarymowycz VA, Stone MJ (2006) Fast time scale dynamics of protein backbones: NMR relaxation methods, applications, and functional consequences. Chem Rev 106:1624–1671

Kay LE (2005) NMR studies of protein structure and dynamics. J Magn Reson 173:193–207

Kay LE, Torchia DA, Bax A (1989) Backbone dynamics of proteins as studied by nitrogen-15 inverse detected heteronuclear NMR spectroscopy: application to staphylococcal nuclease. Biochemistry 28:8972–8979

Kay LE, Nicholson LK, Delaglio F, Bax A, Torchia DA (1992) Pulse sequences for removal of the effects of cross correlation between dipolar and chemical-shift anisotropy relaxation mechanisms on the measurement of heteronuclear T1 and T2 values in proteins. J Magn Reson 97:359–375

Korzhnev DM, Tischenko EV, Arseniev AS (2000) Off-resonance effects in N-15 T-2 CPMG measurements. J Biomol NMR 17:231–237

Li Z, Raychaudhuri S, Wand AJ (1996) Insights into the local residual entropy of proteins provided by NMR relaxation. Protein Sci 5:2647–2650

Lipari G, Szabo A (1982a) Model-free approach to the interpretation of nuclear magnetic resonance relaxation in macromolecules. 1. Theory and range of validity. J Am Chem Soc 104:4546–4559

Lipari G, Szabo A (1982b) Model-free approach to the interpretation of nuclear magnetic resonance relaxation in macromolecules. 2. Analysis of experimental results. J Am Chem Soc 104:4559–4570

Long D, Liu M, Yang D (2008) Accurately probing slow motions on millisecond timescales with a robust NMR relaxation experiment. J Am Chem Soc 130:2432–2433

Loria JP, Rance M, Palmer AG III (1999) A relaxation-compensated Carr-Purcell-Meiboom-Gill sequence for characterizing chemical exchange by NMR spectroscopy. J Am Chem Soc 121:2331–2332

Meiboom S, Gill D (1958) Modified spin-echo method for measuring nuclear relaxation times. Rev Sci Instrm 29:688–691

Mulder FA, van Tilborg PJ, Kaptein R, Boelens R (1999) Microsecond time scale dynamics in the RXR DNA-binding domain from a combination of spin-echo and off-resonance rotating frame relaxation measurements. J Biomol NMR 13:275–288

Myint W, Ishima R (2009) Chemical exchange effects during refocusing pulses in constant-time CPMG relaxation dispersion experiments. J Biomol NMR 45:207–216

Myint W, Gong Q, Ishima R (2009) Practical aspects of 15 N CPMG transverse relaxation experiments for proteins in solution. Concepts Magn Reson 34A:63–75

Nalam MN, Peeters A, Jonckers TH, Dierynck I, Schiffer CA (2007) Crystal structure of lysine sulfonamide inhibitor reveals the displacement of the conserved flap water molecule in human immunodeficiency virus type 1 protease. J Virol 81:9512–9518

Nicholson LK, Kay LE, Baldisseri DM, Arango J, Young PR, Bax A, Torchia DA (1992) Dynamics of methyl groups in proteins as studied by proton-detected 13C NMR spectroscopy. Application to the leucine residues of Staphylococcal nuclease. Biochemistry 31:5253–5263

Nirmala NR, Wagner G (1988) Measurement of C-13 relaxation-times in proteins by two-dimensional heteronuclear H1-C-13 correlation spectroscopy. J Am Chem Soc 110:7557–7558

Orekhov VY, Pervushin KV, Arseniev AS (1994) Backbone dynamics of (1–71)bacterioopsin studied by two-dimensional 1H–15 N NMR spectroscopy. Eur J Biochem 219:887–896

Palmer AG III (2001) Nmr probes of molecular dynamics: overview and comparison with other. Annu Rev Biophys Biomol Struct 30:129–155

Palmer AG III, Rance M, Wright PE (1991) Intramolecular motions of a zinc finger DNA-binding domain from Xfin characterized by proton-detected natural abundance 13C Heteronuclear NMR spectroscopy. J Am Chem Soc 113:4371–4380

Palmer AG III, Skelton NJ, Chazin WJ, Wright PE, Rance M (1992) Suppression of the effects of cross-correlation between dipolar and anisotropic chemical-shift relaxation mechanisms in the measurement of spin spin relaxation rates. Mol Phys 75:699–711

Peng JW, Wagner G (1995) Frequency spectrum of NH bonds in eglin c from spectral density mapping at multiple fields. Biochemistry 34:16733–16752

Redfield C (2004) Using nuclear magnetic resonance spectroscopy to study molten globule states of proteins. Methods Mol Biol 34:121–132

Ross A, Czisch M, King GC (1997) Systematic errors associated with the CPMG pulse sequence and their effect on motional analysis of biomolecules. J Magn Reson 124:355–365

Skelton NJ, Palmer AG III, Akke M, Kordel J, Rance M, Chazin WJ (1993) Practical aspects of 2-dimensional proton-detected N-15 spin relaxation measurements. J Magn Reson, Ser B 102:253–264

Smith LJ, Mark AE, Dobson CM, van Gunsteren WF (1995) Comparison of MD simulations and NMR experiments for hen lysozyme. Analysis of local fluctuations, cooperative motions, and global changes. Biochemistry 34:10918–10931

Szyperski S, Luginbühl P, Otting G, Güntert P, Wüthrich K (1993) Protein dynamics studied by rotating frame. J Biomol NMR 3:151–164

Viles JH, Duggan BM, Zaborowski E, Schwarzinger S, Huntley JJ, Kroon GJ, Dyson HJ, Wright PE (2001) Potential bias in NMR relaxation data introduced by peak intensity analysis and curve fitting methods. J Biomol NMR 21:1–9

Wrabl JO, Shortle D, Woolf TB (2000) Correlation between changes in nuclear magnetic resonance order parameters and conformational entropy: molecular dynamics simulations of native and denatured staphylococcal nuclease. Proteins 38:123–133

Yamasaki K, Saito M, Oobatake M, Kanaya S (1995) Characterization of the internal motions of Escherichia coli ribonuclease HI by a combination of 15 N-NMR relaxation analysis and

molecular dynamics simulation: examination of dynamic models. Biochemistry 34:6587–6601

Yang DW, Kay LE (1996) Contributions to conformational entropy arising from bond vector fluctuations measured from NMR-derived order parameters: application to protein folding. J Mol Biol 263:369–382

Yip GN, Zuiderweg ER (2004) A phase cycle scheme that significantly suppresses offset-dependent artifacts in the R2-CPMG 15 N relaxation experiment. J Magn Reson 171:25–36